Chapter 5

Newtonian dynamics

You might think that the strangeness of contracting flows, flows such as the Rössler flow of fig. 2.3 is of concern only to chemists. Not at all - while it is easier to visualize aperiodic dynamics when the flow is contracting onto a lower-dimensional attracting set, there are plenty examples of chaotic flows that do preserve the full symplectic invariance of Hamiltonian dynamics.

5.1 Hamiltonian flows

An important class of dynamical systems are the Hamiltonian flows, given by a time-independent Hamiltonian $H(q,p)$ together with the Hamilton's equations of motion

appendix C

$$\dot{q}_i = \frac{\partial H}{\partial p_i}\,, \qquad \dot{p}_i = -\frac{\partial H}{\partial q_i}\,, \tag{5.1}$$

with the $2D$ phase space coordinates x split into the configuration space coordinates and the conjugate momenta of a Hamiltonian system with D degrees of freedom:

sect. 26.1.1

$$x = (\mathbf{p}, \mathbf{q})\,, \qquad \mathbf{q} = (q_1, q_2, \ldots, q_D)\,, \qquad \mathbf{p} = (p_1, p_2, \ldots, p_D)\,. \tag{5.2}$$

Example 5.1 Collinear helium. *In chapter 29, we shall apply the periodic orbit theory to the quantization of helium. In particular, we will study* collinear helium, *a doubly charged nucleus with two electrons arranged on a line, an electron on each side of the nucleus. The Hamiltonian for this system is*

chapter 29

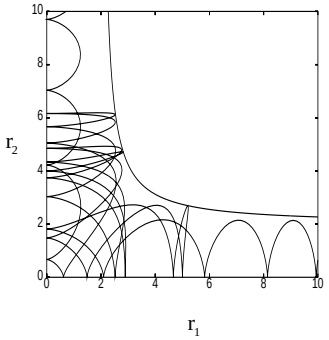

Figure 5.1: A typical colinear helium trajectory in the r_1 – r_2 plane; the trajectory enters here along the r_1 axis and then, like almost every other trajectory, after a few bounces escapes to infinity, in this case along the r_2 axis.

$$H = \frac{1}{2}p_1^2 + \frac{1}{2}p_2^2 - \frac{2}{r_1} - \frac{2}{r_2} + \frac{1}{r_1 + r_2}\,. \tag{5.3}$$

The collinear helium has 2 degrees of freedom, thus a 4-dimensional phase space $\mathcal{M}$, which the energy conservation reduces to 3 dimensions. The dynamics can be visualized as a motion in the (r_1, r_2), $r_i \geq 0$ quadrant, fig. 5.1. It looks messy, and, indeed, it will turn out to be no less chaotic than a pinball bouncing between three disks.

5.1.1 Stability of Hamiltonian flows

As the Hamiltonian flows are so important in physical applications, we digress here to illustrate the ways in which an invariance of equations of motion affects dynamics. In case at hand the *symplectic invariance* will reduce the number of independent stability exponents by factor 2 or 4.

The equations of motion for a time independent D-degrees of freedom Hamiltonian (5.1) can be written as

$$\dot{x}_m = \omega_{mn}\frac{\partial H}{\partial x_n}, \qquad \omega = \begin{pmatrix} 0 & -\mathbf{I} \\ \mathbf{I} & 0 \end{pmatrix}, \qquad m, n = 1, 2, \ldots, 2D \tag{5.4}$$

where $x = [p, q]$ is a phase space point, $\mathbf{I} = [D\times D]$ unit matrix, and ω the $[2D\times 2D]$ *symplectic* form

$$\omega_{mn} = -\omega_{nm}\,, \qquad \omega^2 = -\mathbf{1}\,. \tag{5.5}$$

The linearized motion in the vicinity $x + \delta x$ of a phase space trajectory $x(t) = (p(t), q(t))$ is described by the Jacobian matrix (4.20). The matrix of variations in (4.28) takes form

$$A(x)_{mn} = \omega_{mk}H_{kn}(x)\,, \qquad \frac{d}{dt}\mathbf{J}^t(x) = A(x)\mathbf{J}^t(x)\,, \tag{5.6}$$

where $H_{kn} = \partial_k \partial_n H$ is the Hessian matrix of second derivatives. From (5.6) and the symmetry of H_{kn} it follows that

$$A^T \omega + \omega A = 0\,. \tag{5.7}$$

This is the defining property for infinitesimal generators of *symplectic* (or canonical) transformations, transformations that leave the symplectic form ω_{mn} invariant. From this it follows that for Hamiltonian flows $\frac{d}{dt}\left(\mathbf{J}^T \omega \mathbf{J}\right) = 0$, and that $\mathbf{J}$ is a symplectic transformation (we suppress the dependence on the time and initial point, $\mathbf{J} = \mathbf{J}^t(x_0)$, $\Lambda = \Lambda(x_0, t)$, for notational brevity):

$$\mathbf{J}^T \omega \mathbf{J} = \omega\,. \tag{5.8}$$

The transpose $\mathbf{J}^T$ and the inverse $\mathbf{J}^{-1}$ are related by

$$\mathbf{J}^{-1} = -\omega \mathbf{J}^T \omega\,, \tag{5.9}$$

hence if Λ is an eigenvalue of $\mathbf{J}$, so are $1/\Lambda$, Λ^* and $1/\Lambda^*$. Real (non-marginal) eigenvalues always come paired as Λ, $1/\Lambda$. The complex eigenvalues come in pairs Λ, Λ^*, $|\Lambda| = 1$, or in loxodromic quartets Λ, $1/\Lambda$, Λ^* and $1/\Lambda^*$, so

5.8 page 94

$$\det \mathbf{J}^t(x_0) = 1 \qquad \text{for all } t \text{ and } x_0\text{'s}\,, \tag{5.10}$$

and symplectic flows preserve the *Liouville phase space volume*.

Example 5.2 2-dimensional symplectic flows *In the 2-dimensional case the eigenvalues (4.35) depend only on* $\operatorname{tr} \mathbf{J}^t$

$$\Lambda_{1,2} = \frac{1}{2}\left(\operatorname{tr} \mathbf{J}^t \pm \sqrt{(\operatorname{tr} \mathbf{J}^t - 2)(\operatorname{tr} \mathbf{J}^t + 2)}\right)\,. \tag{5.11}$$

The trajectory is elliptic if the residue $|\operatorname{tr} \mathbf{J}^t| - 2 \leq 0$, *with complex eigenvalues* $\Lambda_1 = e^{i\theta t}$, $\Lambda_2 = \Lambda_1^* = e^{-i\theta t}$. *If* $|\operatorname{tr} \mathbf{J}^t| - 2 > 0$, *the trajectory is* ($\lambda$ *real*)

$$\textit{either}\quad \text{hyperbolic} \qquad \Lambda_1 = e^{\lambda t}\,, \quad \Lambda_2 = e^{-\lambda t}\,, \tag{5.12}$$

$$\textit{or}\quad \text{inverse hyperbolic} \qquad \Lambda_1 = -e^{\lambda t}\,, \quad \Lambda_2 = -e^{-\lambda t}\,. \tag{5.13}$$

in depth: appendix C.1, p. 621

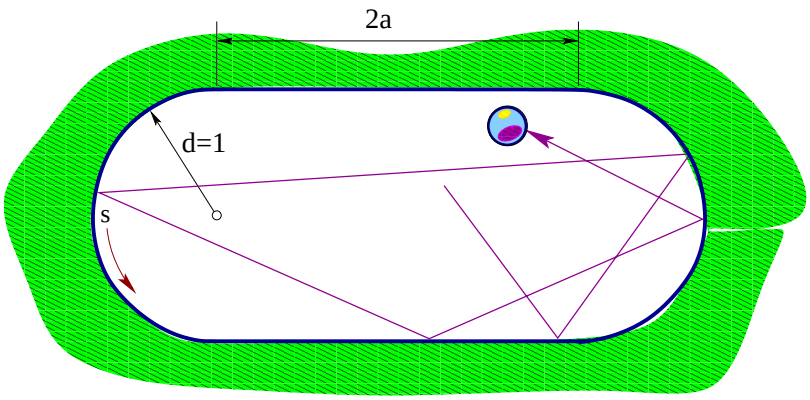

Figure 5.2: The stadium billiard is a 2-dimensional domain bounded by two semi-circles of radius $d = 1$ connected by two straight walls of length $2a$. At the points where the straight walls meet the semi-circles, the curvature of the border changes discontinuously; these are the only singular points of the flow. The length a is the only parameter.

5.2 Billiards

The dynamics that we have the best intuitive grasp on, and find easiest to grapple with both numerically and conceptually, is the dynamics of billiards. For billiards discrete time is altogether natural; a particle moving through a billiard suffers a sequence of instantaneous kicks, and executes a simple motion inbetween, so and there is no need to contrive a Poincaré section. We have already used this system in sect. 1.3 as the intuitively most accessible example of chaos. Here we define billiard dynamics more precisely, anticipating the applications to come.

A billiard is defined by a connected region $Q \subset \mathbb{R}^D$, with boundary $\partial Q \subset \mathbb{R}^{D-1}$ separating Q from its complement $\mathbb{R}^D \setminus Q$. Q can consist of one compact, finite volume component (in which case the billiard phase space is bounded, as for the stadium billiard fig. 5.2), or can be infinite in extent, with its complement $\mathbb{R}^D \setminus Q$ consisting of one or several finite or infinite volume components (in which case the phase space is open, as for the 3-disk pinball game fig. 1.1). In what follows we shall more often than not restrict our attention to *planar billiards*. A point particle ("pinball") of mass m and momentum $p_n = mv_n$ moves freely within the billiard, along a straight line, until it encounters the boundary. There it reflects specularly (*specular* = mirrorlike), with no change in tangential component of momentum, and instantaneous reversal of the momentum component normal to the boundary,

$$p' = p - 2(p \cdot \hat{n})\hat{n}\,,$$

where $\hat{n}$ is a unit vector normal to the boundary ∂Q at the collision point.

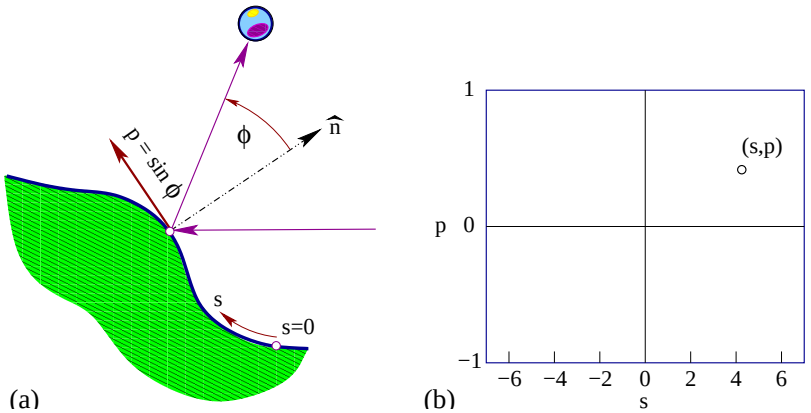

Figure 5.3: (a) A planar billiard trajectory is fixed by specifying the perimeter length parametrized by s and the outgoing trajectory angle ϕ, both measured anti-clockwise with respect to the outward normal $\hat{n}$. (b) The Birkhoff phase space coordinate pair (s, p) fully specifies the trajectory, with $p = \sin\phi$ is the momentum component tangential to the boundary.

The angle of incidence equals to the angle of reflection, fig. 5.3. A billiard is a Hamiltonian system with a $2D$-dimensional phase space $x = (p, q)$ and potential $V(q) = 0$ for $q \in Q$, $V(q) = \infty$ for $q \in \partial Q$.

A billiard flow has a natural Poincaré section defined by marking s_n, the arc length position of the nth bounce measured along the billiard boundary, and $p_n = p\sin\phi_n$, the momentum component parallel to the boundary, where ϕ_n is the angle between the outgoing trajectory and the normal to the boundary. We measure both the arc length s and the parallel momentum p anti-clockwise relative to the outward normal (see fig. 5.3 as well as fig. 1.6a). In $D = 2$, the Poincaré section is a cylinder (topologically an annulus), fig. 5.4, where the parallel momentum p ranges for -1 to 1, and the s coordinate is cyclic along each connected component of ∂Q. The volume in the full phase space is preserved by the Liouville theorem (5.10). The Birkhoff Poincaré section coordinates $x = (s, p) \in \mathcal{P}$, see fig. 5.3, are the natural choice (rather than, let's say, (s, ϕ)), because with them the the Poincaré return map preserves the phase space volume also in the (s, p) parametrized Poincaré section.

5.8
page 94
sect. 5.3

Without loss of generality we will set $m = |v| = |p| = 1$ throughout. Poincaré section condition eliminates one dimension, and the energy conservation $|p| = \text{const.}$ another, hence the Poincaré section return map P is $(2D-2)$-dimensional.

The dynamics is given by the Poincaré return map $P : (s_n, p_n) \mapsto (s_{n+1}, p_{n+1})$ from the nth collision to the $(n+1)$th collision. The discrete time dynamics map P is equivalent to the Hamiltonian flow (5.1) in the sense that both describe the same full trajectory. Let t_n be the instant of

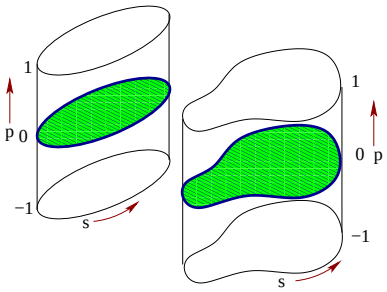

Figure 5.4: In $D = 2$ the billiard Poincaré section is a cylinder, with the parallel momentum p ranging over $p \in \{-1, 1\}$, and with the s coordinate is cyclic along each connected component of ∂Q. The rectangle fig. 5.3(b) is such cylinder unfolded, with periodic boundary conditions glueing together the left and the right edge of the rectangle.

nth collision. Then the position of the pinball $\in Q$ at time $t_n + \tau \leq t_{n+1}$ is given by $2D-2$ Poincaré section coordinates $(s_n, p_n) \in \mathcal{P}$ together with τ, the distance reached by the pinball along the nth section of its trajectory.

Example 5.3 3-disk game of pinball *In case of bounces off a circular disk, the position coordinate $s = r\theta$ is given by angle $\theta \in [0, 2\pi]$. For example, for the 3-disk game of pinball of fig. 1.4 and fig. 1.6 we have two types of collisions:*

5.1 page 93

$$P_0 : \begin{cases} \phi' = -\phi + 2\arcsin p \\ p' = -p + \frac{a}{R}\sin\phi' \end{cases} \qquad \textit{back-reflection} \tag{5.14}$$

$$P_1 : \begin{cases} \phi' = \phi - 2\arcsin p + 2\pi/3 \\ p' = p - \frac{a}{R}\sin\phi' \end{cases} \qquad \textit{reflect to 3rd disk}. \tag{5.15}$$

Here a = radius of a disk, and R = center-to-center separation. Actually, as in this example we are computing intersections of circles and straight lines, nothing more than high-school geometry is required. There is no need to compute arcsin*'s either - one only needs to compute a square root per each reflection, and the simulations can be very fast.*

5.2 page 93

Trajectory of the pinball in the 3-disk billiard is generated by a series of P_0's and P_1's. At each step on has to check whether the trajectory intersects the desired disk (and no disk inbetween). With minor modifications, the above formulas are valid for any smooth billiard as long as we replace a by the local curvature of the boundary at the point of collision.

5.3 Stability of billiards

We turn next to the question of local stability of discrete time systems. Infinitesimal equations of variations (4.2) do not apply, but the multiplicative structure (4.27) of the finite-time Jacobian matrices does. As they are more physical than most maps studied by dynamicists, let us turn to the case of billiards first.

On the face of it, a plane billiard phase space is 4-dimensional. However, one dimension can be eliminated by energy conservation, and the other by

the fact that the magnitude of the velocity is constant. We shall now show how going to the local frame of motion leads to a [2×2] Jacobian matrix.

Consider a 2-dimensional billiard with phase space coordinates $x = (q_1, q_2, p_1, p_2)$. Let t_k be the instant of the kth collision of the pinball with the billiard boundary, and $t_k^{\pm} = t_k \pm \epsilon$, ϵ positive and infinitesimal. With the mass and the velocity equal to 1, the momentum direction can be specified by angle θ: $x = (q_1, q_2, \sin\theta, \cos\theta)$. Now parametrize the 2-$d$ neighborhood of a trajectory segment by $\delta x = (\delta z, \delta\theta)$, where

$$\delta z = \delta q_1 \cos\theta - \delta q_2 \sin\theta\,, \tag{5.16}$$

$\delta\theta$ is the variation in the direction of the pinball. Due to energy conservation, there is no need to keep track of $\delta q_{||}$, variation along the flow, as that remains constant. $(\delta q_1, \delta q_2)$ is the coordinate variation transverse to the kth segment of the flow. From the Hamilton's equations of motion for a free particle, $dq_i/dt = p_i$, $dp_i/dt = 0$, we obtain the equations of motion (4.1) for the linearized neighborhood

$$\frac{d}{dt}\delta\theta = 0, \quad \frac{d}{dt}\delta z = \delta\theta\,. \tag{5.17}$$

Let $\delta\theta_k = \delta\theta(t_k^+)$ and $\delta z_k = \delta z(t_k^+)$ be the local coordinates immediately after the kth collision, and $\delta\theta_k^- = \delta\theta(t_k^-)$, $\delta z_k^- = \delta z(t_k^-)$ immediately before. Integrating the free flight from t_{k-1}^+ to t_k^- we obtain

$$\begin{aligned} \delta z_k^- &= \delta z_{k-1} + \tau_k \delta\theta_{k-1}\,, \qquad \tau_k = t_k - t_{k-1} \\ \delta\theta_k^- &= \delta\theta_{k-1}\,, \end{aligned} \tag{5.18}$$

and the stability matrix (4.26) for the kth free flight segment is

$$\mathbf{J}_T(x_k) = \begin{pmatrix} 1 & \tau_k \\ 0 & 1 \end{pmatrix}\,. \tag{5.19}$$

At incidence angle ϕ_k (the angle between the outgoing particle and the outgoing normal to the billiard edge), the incoming transverse variation δz_k^- projects onto an arc on the billiard boundary of length $\delta z_k^- / \cos\phi_k$. The corresponding incidence angle variation $\delta\phi_k = \delta z_k^- / \rho_k \cos\phi_k$, ρ_k = local radius of curvature, increases the angular spread to

$$\begin{aligned} \delta z_k &= -\delta z_k^- \\ \delta\theta_k &= -\delta\theta_k^- - \frac{2}{\rho_k \cos\phi_k}\delta z_k^-\,, \end{aligned} \tag{5.20}$$

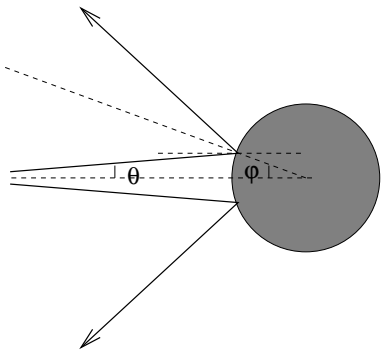

Figure 5.5: Defocusing of a beam of nearby trajectories at a billiard collision. (A. Wirzba)

so the Jacobian matrix associated with the reflection is

$$\mathbf{J}_R(x_k) = -\begin{pmatrix} 1 & 0 \\ r_k & 1 \end{pmatrix}, \qquad r_k = \frac{2}{\rho_k \cos\phi_k}. \tag{5.21}$$

The full Jacobian matrix for n_p consecutive bounces describes a beam of trajectories defocused by $\mathbf{J}_T$ along the free flight (the τ_k terms below) and defocused/refocused at reflections by $\mathbf{J}_R$ (the r_k terms below)

$$\mathbf{J}_p = (-1)^{n_p} \prod_{k=n_p}^{1} \begin{pmatrix} 1 & \tau_k \\ 0 & 1 \end{pmatrix} \begin{pmatrix} 1 & 0 \\ r_k & 1 \end{pmatrix}, \tag{5.22}$$

5.4 page 94

where τ_k is the flight time of the kth free-flight segment of the orbit, $r_k = 2/\rho_k \cos\phi_k$ is the defocusing due to the kth reflection, and ρ_k is the radius of curvature of the billiard boundary at the kth scattering point (for our 3-disk game of pinball, $\rho = 1$). As the billiard dynamics is phase space volume preserving, $\det \mathbf{J} = 1$ and the eigenvalues are given by (5.11).

This is still another example of the Jacobian matrix chain rule (4.31) for discrete time systems, rather similar to the Hénon map stability (4.32). Stability of every flight segment or reflection taken alone is a shear with two unit eigenvalues, but acting in concert in the intervowen sequence (5.22) they can lead to a hyperbolic deformation of the infinitesimal neighborhood of a billiard trajectory.

5.5 page 94

As a concrete application, consider the 3-disk pinball system of sect. 1.3. Analytic expressions for the lengths and eigenvalues of $\overline{0}$, $\overline{1}$ and $\overline{10}$ cycles follow from elementary geometrical considerations. Longer cycles require numerical evaluation by methods such as those described in chapter 14.

5.6 page 94
5.3 page 93
chapter 14

Commentary

Remark 5.1 Billiards. The 3-disk game of pinball is to chaotic dynamics what a pendulum is to integrable systems; the simplest physical example that captures the essence of chaos. Another contender for the title of the "harmonic oscillator of chaos" is the baker's map which is used as the red thread through Ott's introduction to chaotic dynamics [1.7]. The baker's map is the simplest reversible dynamical system which is hyperbolic and has positive entropy. We will not have much use for the baker's map here, as due to its piecewise linearity it is so nongeneric that it misses all of the subtleties of cycle expansions curvature corrections that will be central to this treatise.

chapter 15

That the 3-disk game of pinball is a quintessential example of deterministic chaos appears to have been first noted by B. Eckhardt [3.8]. The model was studied in depth classically, semiclassically and quantum mechanically by P. Gaspard and S.A. Rice [3.9], and used by P. Cvitanović and B. Eckhardt [3.10] to demonstrate applicability of cycle expansions to quantum mechanical problems. It has been used to study the higher order $\hbar$ corrections to the Gutzwiller quantization by P. Gaspard and D. Alonso Ramirez [3.11], construct semiclassical evolution operators and entire spectral determinants by P. Cvitanović and G. Vattay [3.12], and incorporate the diffraction effects into the periodic orbit theory by G. Vattay, A. Wirzba and P.E. Rosenqvist [3.13]. The full quantum mechanics and semiclassics of scattering systems is developed here in the 3-disk scattering context in chapter 28. Gaspard's monograph [1.4], which we warmly recommend, utilizies the 3-disk system in much more depth than will be attained here. For further links check `www.nbi.dk/ChaosBook`.

A pinball game does miss a number of important aspects of chaotic dynamics: generic bifurcations in smooth flows, the interplay between regions of stability and regions of chaos, intermittency phenomena, and the renormalization theory of the "border of order" between these regions. To study these we shall have to face up to much harder challenge, dynamics of smooth flows.

Nevertheless, pinball scattering is relevant to smooth potentials. The game of pinball may be thought of as the infinite potential wall limit of a smooth potential, and pinball symbolic dynamics can serve as a *covering* symbolic dynamics in smooth potentials. One may start with the infinite wall limit and adiabatically relax an unstable cycle onto the corresponding one for the potential under investigation. If things go well, the cycle will remain unstable and isolated, no new orbits (unaccounted for by the pinball symbolic dynamics) will be born, and the lost orbits will be accounted for by a set of pruning rules. The validity of this adiabatic approach has to be checked carefully in each application, as things can easily go wrong; for example, near a bifurcation the same naive symbol string assignments can refer to a whole island of distinct periodic orbits.

sect. 25.1

Remark 5.2 Further reading. The chapter 1 of Gaspard monograph [1.4] is recommended reading if you are interested in Hamilto-

nian flows, and billiards in particular. A. Wirzba has generalized the stability analysis of sect. 5.3 to scattering off 3-dimensional spheres (follow the links in `www.nbi.dk/ChaosBook/extras`). A clear discussion of linear stability for the general d-dimensional case is given in Gaspard [1.4], sect. 1.4.

Résumé

Visualization of strange attractors is greatly facilitated by felicitous choice of Poincaré sections, and reduction of flows to Poincaré section return maps. A particulary natural application of the Poincaré section method is the reduction of a billiard flow to a boundary-to-boundary return map.